Effect of mobility in the rock-paper-scissor dynamics with high mortality

Sahil Islam,[1,*] Argha Mondal,[2,3,†] Mauro Mobilia,[4,‡] Sirshendu Bhattacharyya,[5,§] and Chittaranjan Hens[6,‖]

[1]*Department of Physics, Jadavpur University, Jadavpur, Kolkata 700032, India*
[2]*Department of Mathematics, Sidho-Kanho-Birsha University, Purulia 723104, WB, India*
[3]*Department of Mathematical Sciences, University of Essex, Wivenhoe Park, Colchester CO4 3SQ, United Kingdom*
[4]*Department of Applied Mathematics, School of Mathematics, University of Leeds, Leeds LS2 9JT, United Kingdom*
[5]*Department of Physics, Raja Rammohun Roy Mahavidyalaya, Radhanagar, Hooghly 712406, India*
[6]*Physics and Applied Mathematics Unit, Indian Statistical Institute, Kolkata 700108, India*

(Received 27 November 2021; accepted 11 January 2022; published 27 January 2022)

In the evolutionary dynamics of a rock-paper-scissor model, the effect of natural death plays a major role in determining the fate of the system. Coexistence, being an unstable fixed point of the model, becomes very sensitive toward this parameter. In order to study the effect of mobility in such a system which has explicit dependence on mortality, we perform Monte Carlo simulation on a two-dimensional lattice having three cyclically competing species. The spatiotemporal dynamics has been studied along with the two-site correlation function. Spatial distribution exhibits emergence of spiral patterns in the presence of mobility. It reveals that the joint effect of death rate and mobility (diffusion) leads to new coexistence and extinction scenarios.

DOI: 10.1103/PhysRevE.105.014215

I. INTRODUCTION

A stable ecosystem consists of different coexisting species with naturally balanced intra- and interspecies interactions like offspring production, predation-prey, intrinsic natural death, etc. A natural goal of any ecological system is to maintain the biodiversity such that any species can avoid its extinction. To capture the complexity in a stable ecological system, the principal idea behind evolutionary game dynamics is that the survival or success of species depends on others is very useful [1–6].

A paradigmatic model of evolutionary game dynamics such as the rock-paper-scissor (RPS) model, where cyclic dominance [7–11] determines the fate of each strategy, often successfully mimics the emergence of biodiversity in several natural systems. Colony formation and coexistence of several microbes [8,12–14], parasites [15,16], etc., have been studied using this type of formalism. The stability of the *Uta stansburiana lizards* [17], fermentation in the presence of oxygen and at high glucose concentrations [18], and diversity of coral-reef organisms [19] can be explained with this type of cyclic game. The study of evolutionary RPS model can be characterized [17] in two formalisms: the Lotka-Volterra approach [20–22], in which particular species densities are conserved, and the May-Leonard (ML) approach [23], where vacant sites are introduced and thereby species densities can be varied.

It has already been studied (both theoretically and experimentally) that parameters such as system size, mobility, interaction region, protection spillover, and risk-averse hedgers affect the stability and evolution of the system in a significant manner [4,8,24–28]. In particular, demographic fluctuation breaks the coexistence leading to the extinction of certain species [29–32]. Currently, the role of individual natural death (mortality) has been examined on the cyclic interaction of three species [33]. It is observed that suitable intrinsic death rate of a species may dominate the effect of the birth or predation rates. As a result, a tiny change in the death rate may lead the system toward extinction or make any one species dominate over the others.

On the other hand, mobile species, i.e., species having some kind of exchange or hopping probability may alter the erstwhile scenario of survival [8,34,35]. Depending on the strength of the mobility, several spatial structures such as spiralling pattern [34,36,37] may emerge in the extended two-dimensional (2D) systems. In certain cases, these spirals grow in size depending on the rate of exchange, and after a critical value of the hopping rate, the system shows anomalous behavior where only one species survives and other two go extinct. In particular, the size of spirals expands deliberately and it becomes larger than the system's size enabling any one of those species occupy the whole system [10].

In this backdrop, we revisit the effect of mobility in a cyclic RPS game dynamics where each species has its own intrinsic natural death rate. Using Monte Carlo (MC) simulations [1,38,39], we have explored the effects of mobility in a 2D RPS system within ML formalism where each individual has a mortality rate, i.e., all the species have a probability of death irrespective of any other parameters like predation or reproduction. We have observed that mobility helps the species

*thesahil.islam@gmail.com
†arghamondalb1@gmail.com
‡M.Mobilia@leeds.ac.uk
§Corresponding author: sirs.bh@gmail.com
‖Corresponding author: chittaranjanhens@gmail.com

 ©2022 American Physical Society

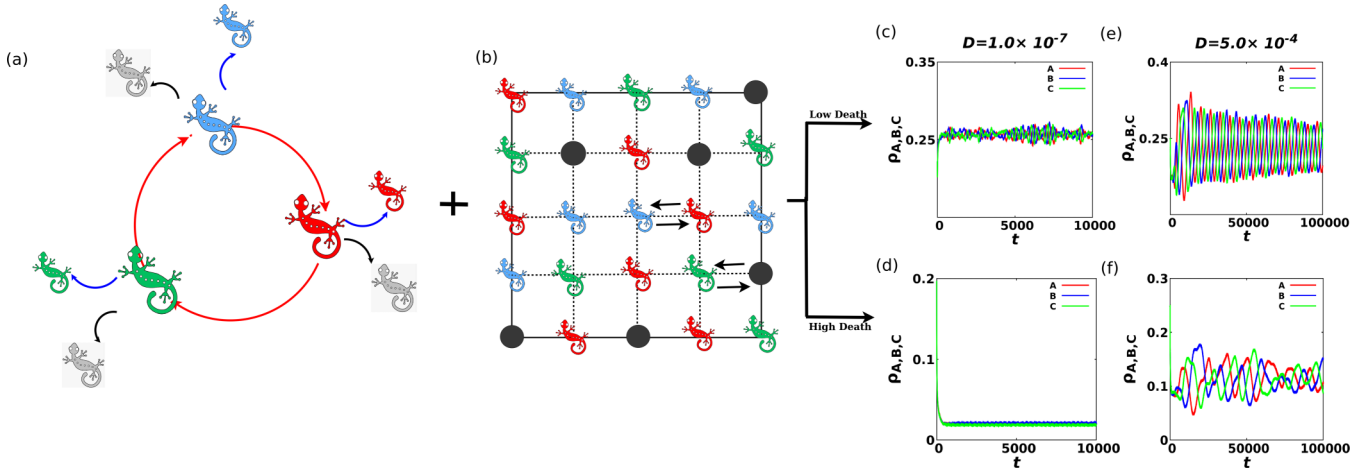

FIG. 1. Schematic diagram of cyclic interaction and mobility in presence of natural death. (a) Red arrows represent the cyclic predation between three species (red, blue, and green). Blue and black arrows reflect the reproduction and natural death respectively. (b) Mobility or exchange between two nearest neighbors (one of them may be vacant site). [(c) and (e)] At low death rate ($d = 1$), the densities of species remain finite for two mobility strength: smaller $D = 1 \times 10^{-7}$ as well as in higher value $D = 5 \times 10^{-4}$. (d) At high death rate ($d = 4$) and for low diffusion, the density of each species is almost zero and no oscillatory behavior is observed there. However, (f) in the presence of higher diffusion, the oscillation with higher amplitude appears. In all the cases, 1000×1000 lattice has been considered with unnormalized predation and reproduction rates, $p = 7$ and $r = 7$, respectively, for each of the species.

survive in an unfavourable environment where mortality rate is high.

The rest of the article is organized as follows. We describe the model, the dynamics, and the method of simulation in Sec. II. The results are discussed in Sec. III and finally we conclude our remarks in Sec. IV.

II. THE FORMULATION OF THE MODEL AND MONTE CARLO SIMULATION

We consider three species in a 2D lattice where each lattice site can either have one species or be vacant. In the beginning of the simulation, the species and vacancies are randomly distributed. Then we perform MC simulation governed by some interactions such as reproduction, predation, natural death, and mobility all subjected to some predefined conditions.

We denote the three species by A, B, and C and the corresponding densities by ρ_a, ρ_b, and ρ_c, respectively. The vacancies are denoted by V and their density by ρ_v where $\rho_a + \rho_b + \rho_c + \rho_v = 1$. In the cyclic domination process, the predations can be represented by the following equations:

$$\begin{aligned} A + B &\longrightarrow A + V \quad \text{with rate} \quad p_a \\ B + C &\longrightarrow B + V \quad \text{with rate} \quad p_b \\ C + A &\longrightarrow C + V \quad \text{with rate} \quad p_c, \end{aligned} \tag{1}$$

where $p_{a,b,c}$ are the predation rates of A, B, and C, respectively. The reproductions can be expressed as

$$\begin{aligned} A + V &\longrightarrow A + A \quad \text{with rate} \quad r_a \\ B + V &\longrightarrow B + B \quad \text{with rate} \quad r_b \\ C + V &\longrightarrow C + C \quad \text{with rate} \quad r_c. \end{aligned} \tag{2}$$

The rate of reproductions are denoted by $r_{a,b,c}$. Alongside, the natural death of a species can make a site vacant as well,

$$S \longrightarrow V \quad \text{with rate} \quad d_{a,b,c}, \tag{3}$$

where S represents any of the three species A, B, or C and V is the vacant site. The corresponding rate of death is d_a, d_b, or d_c. The cyclic predations, reproductions, and deaths are schematically shown in Fig. 1(a). Here red lizards (say, A) predate the greens (B), greens predate the blues (C), and blues predate the reds again. The blue arrows in Fig. 1(a) denote the birth of new species. Each lizard of particular color creates another one of the same color (shown in smaller size). The black arrows indicate the natural death, and the grey lizards indicate the dead ones. Note that we have considered identical predation, reproduction, and death rate of each species: $p_a = p_b = p_c = p$, $r_a = r_b = r_c = r$, and $d_a = d_b = d_c = d$.

Finally, we have considered nearest-neighbor pair exchange where the species can exchange their positions with that of the neighboring species or vacancy governed by some probability:

$$S + \phi(\neq S) \longrightarrow \phi(\neq S) + S \quad \text{with rate} \quad \epsilon. \tag{4}$$

Here ϕ can be A, B, C, or V. Figure 1(b) describes this mobility process. Here one blue and one red lizard in the lattice exchanged their position (marked by thick black arrow). In a similar way, a lizard (see the green one) may hop to a vacant site (described as black filled dots). Note that both swaps (between species-species or species-vacant) do not occur simultaneously but in two different MC step. We consider only nearest neighbor interactions and assume periodic boundary condition while doing the simulation. The simulation starts with a random initial configuration. At each MC step one lattice site is considered randomly. Then another site is chosen out of the four nearest neighbors of the first site and possible operations (predation, reproduction, exchange) are made between two sites with specified probabilities. Apart from this, the chosen first site is converted to a vacant one with death rate d. All the probabilities are normalized by the rates r, p, d, and ϵ. This entire process is repeated until an equilibration is reached. Numerical simulations have been performed on

1000×1000 lattice, and total number of required MC steps varied from 10^4 to 10^6 depending on the rate of mobility. The exchange process in Eq. (4) leads to an effective diffusion of the individual species governed by the macroscopic diffusion constant D. In our case of a two-dimensional system, we connect this diffusion constant D with the exchange rate ϵ through system size by the relation, $\epsilon = 2N^2D$ [40].

III. SIMULATION RESULTS

It has already been established [33] that the system has sharp dependence on natural death as compared to predation and reproduction. For a certain set of parameter values [33] the system also exhibits coexistence of all the species resulting from an unstable fixed point having all nonzero densities. Now, with the incorporation of diffusion (or mobility), the fluctuation expectedly increases in the dynamics. Figures 1(c)–1(f) reports the density of the species with respect to time for two different death rates and two different mobility rates. In lower (higher) death rate, the density of each species shows a stable oscillation with high (small) amplitude. However, the fluctuations are noted to be increased considerably when the mobility rate increases from 1.0×10^{-7} [Figs. 1(c) and 1(d)] to 5.0×10^{-4} [Figs. 1(e) and 1(f)]. Increase of mobility rate is observed to affect the average densities of the species significantly in the regime of high as well as low death rate. When death rate is high the average species densities remain very low, leaving most of the lattice sites vacant for low mobility [e.g., see Fig. 1(d) for $d = 4$]. However, an increasing value of diffusion enhances the species densities for the same rate of death. We can see in Fig. 1(f) that the average density of the species has been raised as mobility becomes 5.0×10^{-4}. The situation becomes opposite when we are in the low death regime. Increasing mobility lowers the species densities there. This feature indicates that a coexistence regime may arise under high death rates within a critical boundary of mobility We explore the combined effect of death rates and mobility for finding the coexistence as well as the the extinction regime.

To delve deeper, we have calculated the total density of species $(1 - \rho_v)$ in the lattice as a function of mobility strength for different death rates. The time-averaged total density is calculated following the definition

$$\rho_{\text{total}} = \frac{1}{t_f - t_i} \sum_{t_i}^{t_f} (\rho_a + \rho_b + \rho_c), \tag{5}$$

where both t_i and t_f are in the equilibrated region of the MC simulation. Figure 2(a) shows the plots of ρ_{total} against mobility rate for six different death rates. At lower mobility ($D \sim 10^{-7}$) and low death rates ($d = 0$ and $d = 1$, i.e., purple and green lines), the three species collectively occupy around 90% and 80% space of the whole lattice, respectively. When the mobility rate increases, ρ_{total} decreases continuously and saturates at certain values (∼0.8 for purple and ∼0.7 for green line). The total density remains almost unaltered with varying mobility for moderate death rates ($d \sim 2$). On the other hand, for species with higher death rates ($d \gtrsim 3$), an increase in ρ_{total} is observed with increasing mobility rate. For very high death rate ($d \sim 5$), coexistence of species is observed. By contrast,

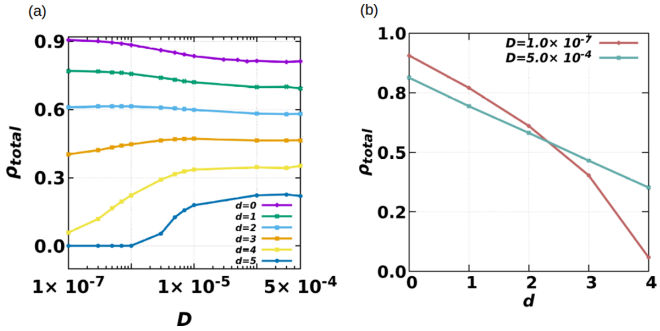

FIG. 2. Role of mobility and death rate on species coexistence. (a) Total species densities are plotted against mobility strength (D) for six constant death rates. We observe that at lower death rates as the mobility increases the total species density decreases slowly. At high death rate and low mobility the species density is very low (gets extinct for $d = 5$). However, as the mobility increases species density increases ("revives" even for $d = 5$) and coexists. (b) Total species density is plotted for two extreme mobility constants ($D = 1.0 \times 10^7$ and $D = 5.0 \times 10^{-4}$) with increasing death rate. With increasing death rate, the total species density decreases, but the slope for these two cases are different. Lower mobility leads to faster extinction but higher mobility decreases the slope and leads to nonextinction of the species for a wider range of death rate.

the system shows extinction at low diffusion. In Fig. 2(b), we have plotted the total species density as a function of death rates for two extreme mobility strengths ($D = 1.0 \times 10^{-7}$ and $D = 5.0 \times 10^{-4}$). We observe a monotonic decrease of ρ_{total} with the death rate d. As the figure shows that the lower mobility rate (magenta line) has faster decay in ρ_{total} than the higher mobility case (green line). This leads to the fact that the system with higher mortality can overcome extinction for certain range of higher mobility value. Additionally, we observe a crossover of the two lines where the total density is around 0.55. This intersection point gives a certain value of death rate and species density where two extreme mobility rates lead to an identical population density.

For further analysis, we have plotted the species density spatially in a 1000×1000 lattice (Fig. 3). Each of the figure is plotted when the system had already reached stable oscillation well ahead. In the first row, where no natural death rate is considered, the size of the spirals increase from low mobility to higher mobility ($D = 1.0 \times 10^{-7}$ to $D = 1 \times 10^{-4}$). If we increase the mobility rate further ($D \geqslant 7.0 \times 10^{-4}$), then the size of one spiral would be inflated so much that it would occupy the entire lattice leading to the situation of single species survival (not shown here). This is consistent with the previously reported results [10]. Now, if we introduce the natural death of each species, then the size of the spirals grow more rapidly (second row, from left to right). In the third row, at death rate $d = 4$ and at mobility strength $D = 1 \times 10^{-7}$ a large fraction of the lattice sites become vacant. Thus a large collection of black dots appear in the spatial plot. However, if we increase D, then the large spirals reappear in the lattice. Panels of two bottom rows, for $d = 4$ and $d = 5$, become less dark as D is increased (left to right). Thus, the mobility has capability of countering the effect of death rate of the species.

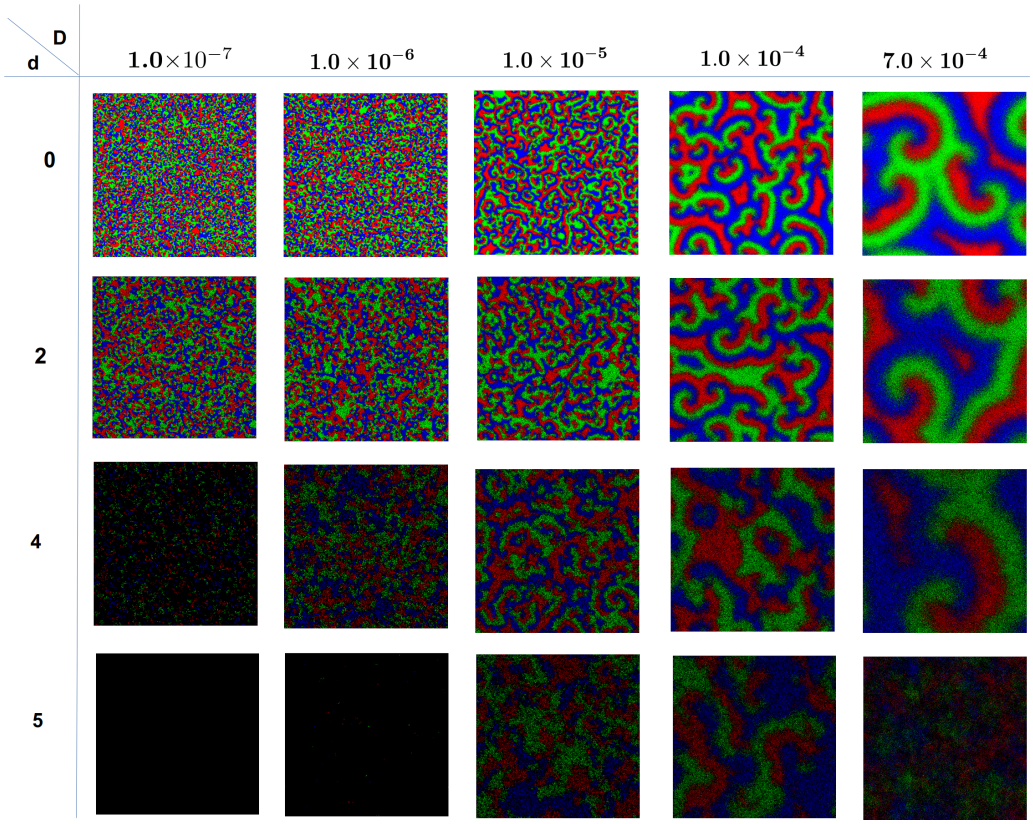

FIG. 3. Spatial plot of species density for different death rate and mobility strength. Distribution of the species throughout the lattice is shown by colors (red, green, and blue for A, B, and C, respectively). Black dots are used for blank space. Diffusion strength is increased from 10^{-7} to 7×10^{-4} (from left to right). Natural death rate is increased from zero to 5 (upper to bottom).

The mathematical analysis of the emergence of spiral patterns [41–46] will be explored in future.

The patterns can also be realized from the study of the spatial correlation. The two-site correlation function is defined by:

$$g_{s_i s_j}(\mathbf{r}-\mathbf{r}',t) \equiv \langle s_i(\mathbf{r},t)s_j(\mathbf{r}',t)\rangle - \langle s_i(\mathbf{r},t)\rangle\langle s_j(\mathbf{r}',t)\rangle. \quad (6)$$

Here $s_{i,j}(\mathbf{r},t)$ $(i,j\in a,b,c)$ represents a species at the position $\mathbf{r}$ in the 2D lattice at a particular time t [40]. We study the correlation of species A ($g_{s_a s_a}$) and it shows damped oscillation with respect to distance in case of the spiral patterns as observed in earlier studies [40,47]. The correlation length ($l_{\rm corr}$) is thereby determined by the length at which the correlation drops $1/e$th of the maximum value [34]. As expected [10], all the plots show that the correlation length increases with increasing mobility indicating the size of a single patch in the spatial distribution getting bigger. At lower diffusion, the correlation length for high death rate is almost nil mainly due to the extinction of species at that regime [Fig. 4(a)]. At higher mobility ($D\sim10^{-5}$) a new coexistence regime appears (the blue and yellow line, also see the third and fourth row of the Fig. 3) significantly boosts up the correlation length curve jointly with the inflated spiral size. The size of the spiral increases with the death rate as well. This is indicated by Fig. 4(b) where we have plotted the wavelength (λ) of the correlation function ($g_{s_a s_a}$) against death rates.

Interestingly in the regime of high diffusion, the growth of the correlation length, i.e., the size of the patch is elevated and the significance is that the species are prone to colony formation more when their mortality rates are high. This feature will be explored in more details in future.

We have also calculated the extinction probability [$P_{\rm ext}$, Fig. 4(c)] against mobility strength for different death rates. Here $P_{\rm ext}$ is the probability of extinction of one or more species [10], numerically calculated over a large number of realizations for a lattice size of 1000×1000 and for 10^6 MC steps. It is already established that [10] an abrupt transition occurs from coexistence to extinction (size $N\to\infty$) above a certain critical D in the case of $d=0$. In finite systems, there are finite-size effects as shown in Fig. 4(b) (blue, red, and green). For higher mobility ($D>10^{-3}$), the coexistence is completely lost, as the patch of one species becomes big enough to cover the entire space. The results are almost same for death rates $d=2$ (brown) and $d=4$ (green). In the presence of death, the system reaches extinction at smaller diffusion compared to zero mortality rate. However, an interesting feature is observed for higher mortality rates. For large d [$d=5$ (yellow) and $d=6$ (violet)], new extinction and coexistence regimes appear that is characterized by two critical values of D: D_{c1} and D_{c2}. For $D<D_{c1}$ and $D>D_{c2}$ one species takes over, and coexistence is lost after a time of order N (effect of lattice size is explored in Fig. 5). For $D_{c1}<D<D_{c2}$ long-lived coexistence of all species (metastable state) occurs for a time that grows exponentially with N (Fig. 5). For instance, at $d=5$, there is only one surviving species for $D\lesssim10^{-5}$ and $D\gtrsim10^{-3}$ and species coexist for

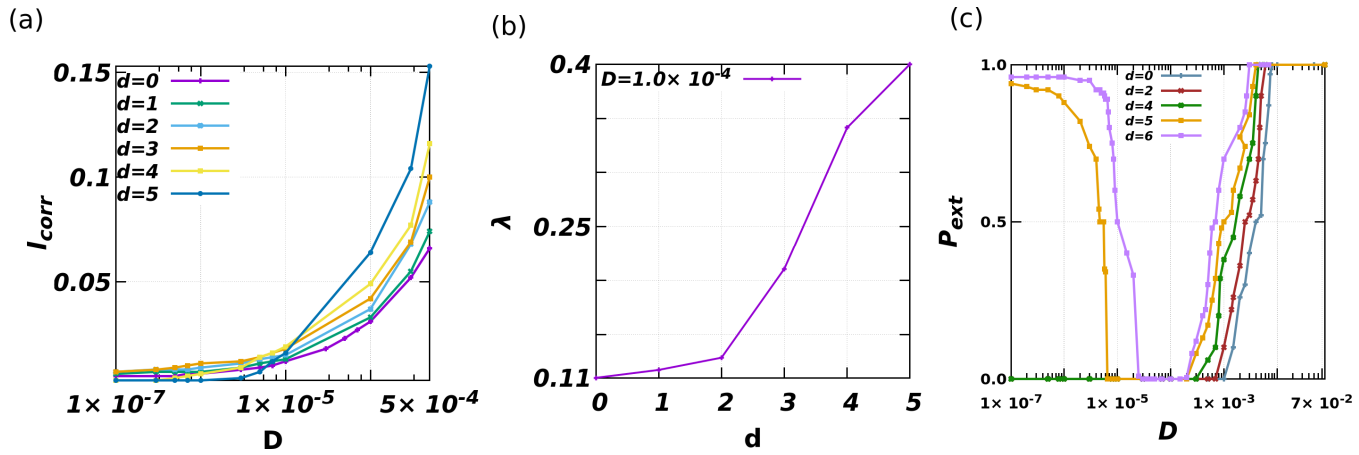

FIG. 4. (a) Correlation lengths ($l_{\rm corr}$) are plotted against different mobility strengths (D). At higher diffusion, the length is enhanced. This is consistent with previous results [10]. If the death rate is increased, then the length is also sharply increased. In intermediate mobility strength ($D \sim 10^{-5}$), the species density "revives" (species coexistence) for higher death rate thus correlation becomes nonzero (see the blue and yellow lines). (b) The wavelength (λ) of the correlation function as a function of death (d) for a particular value of mobility ($D = 1.0 \times 10^{-4}$). The wavelength is increasing as we increase the death value. This indicates the spirals increase in size with increasing death rate. (c) Extinction probability as a function of mobility D. Five death rates have been chosen. For higher death rates ($d = 5, 6$), the extinction probability is high for low ($D \sim 10^{-7}$) and high ($D \gtrsim 10^{-3}$) diffusion and goes to zero in the intermediate values of $D \sim 10^{-4}$.

$10^{-5} < D < 10^{-3}$. Here the joint effect of high death rate and mobility leads to new extinction and coexistence regimes or scenarios. Below we provide an intuitive interpretation of these findings. Note that we have confirmed this scenario and the values of $P_{\rm ext}$, D_{c1}, and D_{c2}, for larger systems in order to rule out the influence of finite-size effects.

When d is large, there are numerous spontaneous death events leading to a lot of empty spaces. Moreover, when there is enough mobility (high D), individuals visit a large fraction of the lattice and hence can efficiently find available empty sites where to reproduce before being killed. In this sense high mobility rate D counters high death rates and allows species to coexist under extreme conditions (high d) provided that they are sufficiently mobile (high-enough D). Of course, if D is too large, then spiralling patterns just outgrow the system as in Ref. [10]. When d is small, we also recover essentially the same extinction-coexistence scenario as in Ref. [10].

Novel phenomenology hence arises when d is large and D is sufficiently large (but not too large); mobility counters the effect of killing and allows species to coexist for a very long time (see below and Fig. 5). In the opposite limit, when D is small (d being large), individuals are not mobile enough to escape spontaneous death and species coexistence ceases after a finite time.

Finally, we have investigated the effect of finite size in the dynamics. We have chosen four death rates: $d = 0, 2, 4,$ and 5. The average extinction time $\langle T_{\rm ex}\rangle$ of the species is plotted with the system size N [Figs. 5(a)–5(d)]. The extinction time ($T_{\rm ex}$) is measured when one of the species goes to extinction. For each death rate and diffusion, the average extinction time, $\langle T_{\rm ex}\rangle$ is calculated for 100 realizations (1 time step $= N$ Monte Carlo steps $= N$ update moves). The mean extinction time $\langle T_{\rm ex}\rangle$ increases with increasing system size and the nature of the curve depends on the strength of mobility as observed previously in absence of any death

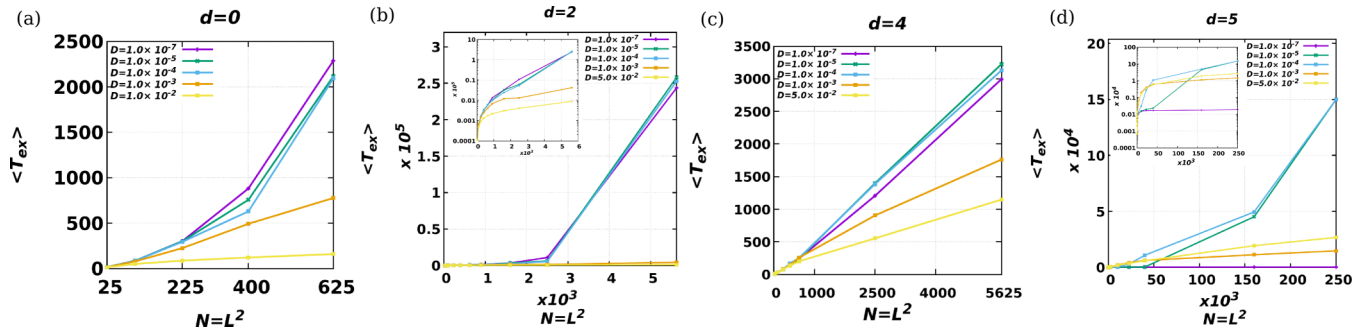

FIG. 5. Effect of lattice size on average extinction time at different death rates and mobility parameters: $\langle T_{\rm ex}\rangle$ is plotted against lattice size, $N\ (= L^2)$ for different death rates (d) and mobility (D). [(a)–(b)] Diffusion dominates for low death rates as it lowers the extinction time. [(c) and (d)] For high death rates both low and high diffusivity show lower extinction times, whereas $\langle T_{\rm ex}\rangle$ is raised for an intermediate range of diffusion. Note that in (d) data for $d = 5, N = 500^2$, and $D = 10^{-4}$ and $D = 10^{-5}$ are given as eye guides since coexistence is not lost at time 1.5×10^5 (hence, in these cases $\langle T_{\rm ex}\rangle > 1.5 \times 10^5$), see text. Insets of (b) and (d): $\langle T_{\rm ex}\rangle$ vs. N on lin-log scale. In this work, in one time step there are N elementary update moves corresponding to $N = L^2$ Monte Carlo steps.

rate [47]. The death rate also has influence on $\langle T_{ex} \rangle$. In the case of low (or no) death rates [Figs. 5(a) and 5(b)], low mobility is observed to lower the extinction time. For instance, $d = 2$, $P_{ext} \approx 1$ at $D > 10^{-3}$, and $P_{ext} \approx 0$ for $D < 10^{-3}$. This suggests that for $d = 2$ and $D < 10^{-3}$ the coexistence is metastable and extinction occurs in a time that appears to be scaling exponentially with N, as suggested by Fig. 5(b) [see the inset of Fig. 5(b)]. On the other hand, when $D > 10^{-3}$ the systems settles rapidly in a regime where two species have gone extinct and $\langle T_{ex} \rangle$ seems to be approximately linear in N when $N \gg 1$, as in Ref. [47]. In the coexistence-extinction scenario found here, coexistence is metastable at large d and sufficiently large D, e.g., for $d = 5$ and $D = 10^{-5}$–10^{-4}, a regime in which $P_{ext} \approx 0$ and all species coexist for a time that appears to be scaling exponentially with N, see Fig. 5(d) and its inset. Note, however, that for the data point in Fig. 5(d), for $N = 500 \times 500$, with $d = 5$, $D = 10^{-4}$, and $D = 10^{-5}$, simulations were performed for 1.5×10^5 time steps after which species coexistence persists, from which we infer that in these cases $\langle T_{ex} \rangle > 1.5 \times 10^5$, which appears to be compatible with $\langle T_{ex} \rangle$ growing exponentially with N when $N \gg 1$. However, at fixed large d, when D is either very high or too low, e.g., for $D = 10^{-7}$ and $D \gtrsim 10^{-3}$ in Fig. 5(d), $P_{ext} \approx 1$. In these regimes of very low or high D, two species go extinct on a much shorter timescale, with $\langle T_{ex} \rangle$ that appears to grow approximately linearly in N when $N \gg 1$.

IV. CONCLUSION

We study the role of mobility in the spatiotemporal behavior of a three-species ecosystem with cyclically dominating interaction. We also incorporate a rate of natural death which represent the finite lifetime of the living system. The ecosystem is mapped into a two-dimensional lattice on which the RPS dynamics is studied in ML formalism through Monte Carlo simulation. We mainly concentrate in the parameter region where the system exhibits coexistence. The natural death rate has already been proven to affect the coexistence significantly. Our present study reveals that high mobility rate overshadows the act of natural death. We have demonstrated how the time-averaged total density of the competing species changes with the rate of death as well as the rate of diffusion. In addition, the spatiotemporal analysis followed by the two-site correlation length suggests that the size of the patches formed by individual species increases with both D and d. Interestingly, an atypical extinction and coexistence regimes appear under high death rates and are characterized by two critical mobility rates between which species coexist.

In fact, high death rate leads to an increase of vacant sites, leading to more opportunity for random mixing than when $d = 0$. Again the increase of correlation with the death rate suggests that increasing d at fixed D would lead to larger patches of activities but with blurrier shapes and interfaces due to more random mixing. The results therefore suggest that an ecosystem with its constituent species being highly mobile can evade possible extinction caused by increased mortality rate. It has recently been shown that the introduction of pestilent species attacking over a single species may jeopardize the stability of the coexistence [48]. We would like to explore this feature in the presence of natural death and mobility. Moreover, de Oliveira *et al.* [49] have checked the effect of mobility in a lattice of living organisms [50]. Instead of global restrictions on reproduction and movement, these authors considered local restrictions and showed that these were able to generate multicluster states. In future we would like to explore the effect of breaking the directional symmetry of the movement on the appearance of the original coexistence and the extinction scenario.

A diffusive system system allows interspecies exchange which eventually promotes colony formation among the species. However, the influence of mobility in the effect of death rate is counterintuitive because mobility and mortality, as incorporated in this system, are apparently two unconnected phenomena.

ACKNOWLEDGMENT

C.H. is supported by INSPIRE-Faculty grant (Code: IFA17-PH193).

[1] G. Szabó and G. Fath, Phys. Rep. **446**, 97 (2007).
[2] M. Perc, J. J. Jordan, D. G. Rand, Z. Wang, S. Boccaletti, and A. Szolnoki, Phys. Rep. **687**, 1 (2017).
[3] A. Szolnoki, M. Mobilia, L.-L. Jiang, B. Szczesny, A. M. Rucklidge, and M. Perc, J. R. Soc. Interface **11**, 20140735 (2014).
[4] E. Pennisi, Science **309**, 90 (2005).
[5] M. Mobilia, A. M. Rucklidge, and B. Szczesny, Games **7**, 24 (2016).
[6] A. Traulsen, M. A. Nowak, and J. M. Pacheco, Phys. Rev. E **74**, 011909 (2006).
[7] A. Arunachalam, Wireless Pers. Commun. **113**, 1315 (2020).
[8] B. Kerr, M. A. Riley, M. W. Feldman, and B. J. Bohannan, Nature (London) **418**, 171 (2002).
[9] J. Park, Europhys. Lett. **126**, 38004 (2019).
[10] T. Reichenbach, M. Mobilia, and E. Frey, Nature (London) **448**, 1046 (2007).
[11] T. Hashimoto, K. Sato, G. Ichinose, R. Miyazaki, and K.-i. Tainaka, J. Phys. Soc. Jpn. **87**, 014801 (2018).
[12] P.-J. Ke and J. Wan, Ecol. Monogr. **90**, e01391 (2020).
[13] B. Momeni, L. Xie, and W. Shou, Elife **6**, e25051 (2017).
[14] J. R. Nahum, B. N. Harding, and B. Kerr, Proc. Natl. Acad. Sci. USA **108**, 10831 (2011).
[15] D. D. Cameron, A. White, and J. Antonovics, J. Ecol. **97**, 1311 (2009).
[16] A. M. Segura, C. Kruk, D. Calliari, F. García-Rodriguez, D. Conde, C. E. Widdicombe, and H. Fort, Sci. Rep. **3**, 1037 (2013).
[17] B. Sinervo and C. M. Lively, Nature (London) **380**, 240 (1996).
[18] T. Pfeiffer and A. Morley, Front. Mol. Biosci. **1**, 17 (2014).

[19] J. Jackson and L. Buss, Proc. Natl. Acad. Sci. USA **72**, 5160 (1975).
[20] N. Bacaër, in *A Short History of Mathematical Population Dynamics* (Springer, Berlin, 2011), pp. 71–76.
[21] A. J. Lotka, Proc. Natl. Acad. Sci. USA **6**, 410 (1920).
[22] V. Volterra, Nature **118**, 558 (1926).
[23] C.-W. Chi, L.-I. Wu, and S.-B. Hsu, SIAM J. Appl. Math. **58**, 211 (1998).
[24] E. Frey, Physica A **389**, 4265 (2010).
[25] Ana Paula O. Müller and J. A. C. Gallas, Phys. Rev. E **82**, 052901 (2010).
[26] A. Szolnoki and M. Perc, New J. Phys. **17**, 113033 (2015).
[27] E. D. Kelsic, J. Zhao, K. Vetsigian, and R. Kishony, Nature (London) **521**, 516 (2015).
[28] H. Guo, Z. Song, S. Geček, X. Li, M. Jusup, M. Perc, Y. Moreno, S. Boccaletti, and Z. Wang, J. R. Soc. Interface **17**, 20190789 (2020).
[29] T. Reichenbach, M. Mobilia, and E. Frey, Phys. Rev. E **74**, 051907 (2006).
[30] S. R. Serrao, T. Ritmeester, and H. Meyer-Ortmanns, J. Phys. A: Math. Theor. **54**, 235001 (2021).
[31] R. West and M. Mobilia, J. Theor. Biol. **491**, 110135 (2020).
[32] M. Berr, T. Reichenbach, M. Schottenloher, and E. Frey, Phys. Rev. Lett. **102**, 048102 (2009).
[33] S. Bhattacharyya, P. Sinha, R. De, and C. Hens, Phys. Rev. E **102**, 012220 (2020).
[34] T. Reichenbach, M. Mobilia, and E. Frey, J. Theor. Biol. **254**, 368 (2008).
[35] B. C. Kirkup and M. A. Riley, Nature (London) **428**, 412 (2004).
[36] P. P. Avelino, D. Bazeia, L. Losano, J. Menezes, and B. F. Oliveira, Phys. Rev. E **86**, 036112 (2012).
[37] P. P. Avelino, D. Bazeia, L. Losano, J. Menezes, B. F. de Oliveira, and M. A. Santos, Phys. Rev. E **97**, 032415 (2018).
[38] C. Z. Mooney, *Monte Carlo Simulation* (Sage, Thousand Oaks, CA, 1997), p. 116.
[39] E. Zio, in *The Monte Carlo Simulation Method for System Reliability and Risk Analysis* (Springer, Berlin, 2013), pp. 19–58.
[40] T. Reichenbach, M. Mobilia, and E. Frey, Phys. Rev. Lett. **99**, 238105 (2007).
[41] M. Ipsen, F. Hynne, and P. Sørensen, Physica D **136**, 66 (2000).
[42] M. Ipsen, L. Kramer, and P. G. Sørensen, Phys. Rep. **337**, 193 (2000).
[43] Y. Gong and D. J. Christini, Phys. Rev. Lett. **90**, 088302 (2003).
[44] A. Mondal, S. K. Sharma, R. K. Upadhyay, M. A. Aziz-Alaoui, P. Kundu, and C. Hens, Phys. Rev. E **99**, 042307 (2019).
[45] B. Szczesny, M. Mobilia, and A. M. Rucklidge, Phys. Rev. E **90**, 032704 (2014).
[46] A. Mondal, A. Mondal, S. Kumar Sharma, R. Kumar Upadhyay, and C. G. Antonopoulos, Chaos **31**, 103122 (2021).
[47] Q. He, M. Mobilia, and U. C. Täuber, Eur. Phys. J. B **82**, 97 (2011).
[48] D. Bazeia, M. Bongestab, B. de Oliveira, and A. Szolnoki, Chaos Solitons Fract, **151**, 111255 (2021).
[49] B. de Oliveira, M. de Moraes, D. Bazeia, and A. Szolnoki, Physica A **572**, 125854 (2021).
[50] K. Drescher, C. D. Nadell, H. A. Stone, N. S. Wingreen, and B. L. Bassler, Curr. Biol. **24**, 50 (2014).